

Engineering $SU(1, 1) \otimes SU(1, 1)$ vibrational states

C. Huerta Alderete,^{1,*} M. P. Morales Rodríguez,² and B. M. Rodríguez-Lara^{1,3,†}

¹*Instituto Nacional de Astrofísica, Óptica y Electrónica,*

Calle Luis Enrique Erro No. 1, Sta. Ma. Tonantzintla, Pue. CP 72840, México

²*Academia Mexicana de Ciencias, Verano de la*

Investigación Científica – Instituto Nacional de Astrofísica,

Óptica y Electrónica, Calle Luis Enrique Erro No. 1,

Sta. Ma. Tonantzintla, Pue. CP 72840, México

³*Tecnologico de Monterrey, Escuela de Ingeniería y Ciencias,*

Ave. Eugenio Garza Sada 2501, Monterrey, N.L., México, 64849.

(Dated: December 15, 2024)

Abstract

We propose an ideal scheme for preparing vibrational $SU(1, 1) \otimes SU(1, 1)$ states in a two-dimensional ion trap using red and blue second sideband resolved driving of two orthogonal vibrational modes. Symmetric and asymmetric driving provide two regimes to realize quantum state engineering of the vibrational modes. In one regime, we show that time evolution synthesizes so-called $SU(1, 1)$ Perelomov coherent states, that is separable squeezed states and their superposition too. The other regime allows engineering of lossless 50/50 $SU(2)$ beam splitter states that are entangled states. These ideal dynamics are reversible, thus, the non-classical and entangled states produced by our schemes might be used as resources for interferometry.

* e-mail: aldehuer@inaoep.mx

† e-mail: bmlara@itesm.mx

I. INTRODUCTION

Quantum state engineering studies the preparation, manipulation, and characterization of arbitrary quantum states. Technological advances allow the coherent control of dynamics in an increasing collection of physical systems; e.g. trapped ions, superconducting circuits, quantum gases, mechanical oscillators. In particular, trapped ions show high addressability, long coherence times and high fidelity readout necessary for quantum state preparation and manipulation within its own experimental issues [1]. Vibrational state characterization is available through tomographic reconstruction, experimentally demonstrated for Wigner [2] and Husimi [3] quasi-probability distributions.

Trapped ions have proved a fertile ground for fundamental research and quantum technologies development [4, 5]. Single-mode vibrational number, coherent, and squeezed states have been engineered experimentally [6] and theoretical proposals for the synthesis of arbitrary one-[7] and two-dimensional vibrational states [8] has been produced. In particular, trapped ions might act as vibrational beam splitters [9] producing states identical to the photon states on the output ports of a lossless interferometer with number-state inputs [10]. Vibrational interferometry can be used to either explore fundamental quantum mechanics, e.g. quantum decoherence [11, 12], or produce new quantum technologies, e.g. vibrational thermometers [13] or quantum gyroscopes [14].

Squeezing and entanglement improve phase sensitivity in interferometry in a manner proportional to the inverse of the excitation number of quanta entering an interferometer [15–17]. Here, we are interested in the quantum state engineering of orthogonal vibrational modes that show squeezing and entanglement with an underlying $SU(1,1) \otimes SU(1,1)$ symmetry. We will use blue and red resolved second sideband driving [18, 19] to this end. In the following, we will present an effective Hamiltonian describing our proposal in the Lamb-Dicke regime. Then, we will show that the asymmetric coupling model produces the superposition of separable squeezed vibrational mode states where the inner state is intrinsically entangled to the vibrational modes. Afterward, we will show that red driving with symmetric coupling is able to produce lossless 50/50 $SU(2)$ beam splitter vibrational states that are factorized from the internal state of the ion. The ideal dynamics producing these states are reversible and seem to suggest their use as interferometers to characterize different aspects of real-world experiments.

II. DUAL-MODE, SECOND-SIDEBAND DRIVING MODEL

We suggest driving two normal phonon modes of the center of mass motion of a trapped ion [20, 21], such that the effective Hamiltonian,

$$\hat{H}_{ion} = \frac{\omega_0}{2} \hat{\sigma}_3 + \sum_{j=1}^2 \nu_j \hat{a}_j^\dagger \hat{a}_j + \Omega_j \cos \left[\eta_j \left(\hat{a}_j^\dagger + \hat{a}_j \right) - \omega_j t + \phi_j \right] \hat{\sigma}_j, \quad (1)$$

describes the interaction of the j -th vibrational mode, with frequency ν_j and represented by the annihilation (creation) operator \hat{a}_j (\hat{a}_j^\dagger), with two internal levels of the trapped ion, with energy gap ω_0 and represented by Pauli matrices $\hat{\sigma}_j$, through a set of external driving fields of frequency ω_j , Lamb-Dicke parameter η_j , phase ϕ_j , and Rabi coupling strength Ω_j . Moving into the reference frame defined by the uncoupled Hamiltonian, $\hat{H}_0 = \omega_0 \hat{\sigma}_3/2 + \nu_1 \hat{a}_1^\dagger \hat{a}_1 + \nu_2 \hat{a}_2^\dagger \hat{a}_2$, driving the k -th vibrational sideband, $\omega_j = \omega_0 - k\nu_j$ where $k > 0$ and $k < 0$ define the so-called red and blue driving, in the Lamb-Dicke regime, $\eta_j \sqrt{\langle \hat{a}_j^\dagger \hat{a}_j \rangle} \ll 1$, and under an optical and mechanical rotating wave approximation, we can approximate [22] for red,

$$\hat{H}_R \approx \sum_{j=1}^2 \frac{g_{j,k}}{2} \left[e^{i\phi_{j,k}} \hat{a}_j^k \hat{\sigma}_+ + e^{-i\phi_{j,k}} \hat{a}_j^{\dagger k} \hat{\sigma}_- \right], \quad (2)$$

and blue sideband driving,

$$\hat{H}_B \approx \sum_{j=1}^2 \frac{g_{j,k}}{2} \left[e^{i\phi_{j,k}} \hat{a}_j^{\dagger |k|} \hat{\sigma}_+ + e^{-i\phi_{j,k}} \hat{a}_j^{|k|} \hat{\sigma}_- \right], \quad (3)$$

with effective couplings and phases, $g_{j,k} \approx \Omega_j \eta_j^{|k|} e^{-|\eta_j|^2/2}/|k|!$ and $e^{i\phi_{j,k}} = (-i)^{j-1+|k|} e^{i\phi_j}$, in that order. For reasons that will become obvious, we choose the second sideband driving [19], $k = \pm 2$, and draw from the idea of simultaneous blue and red driving in the simulation of the quantum Rabi model [23, 24] to reach the model Hamiltonian at the core of our proposal,

$$\hat{H} = \sum_{j=1}^2 \frac{g_{j,2}}{2} \left[e^{i\phi_{j,2}} \hat{a}_j^2 \hat{\sigma}_+ + e^{-i\phi_{j,2}} \hat{a}_j^{\dagger 2} \hat{\sigma}_- \right] + \frac{g_{j,-2}}{2} \left[e^{i\phi_{j,-2}} \hat{a}_j^{\dagger 2} \hat{\sigma}_+ + e^{-i\phi_{j,-2}} \hat{a}_j^2 \hat{\sigma}_- \right]. \quad (4)$$

This model is the two-photon interaction analog of the so-called cross-cavity quantum Rabi model [25] that has been used to propose the quantum simulation of para-oscillators in trapped ions [26, 27].

III. ASYMMETRIC SQUEEZING

Let us simplify and find uses for our general Hamiltonian. First, we propose to work with a system where the amplitudes and relative phases for blue and red driving in each mode are chosen to provide similar coupling parameters, $g_{j,k} \equiv g_j$, and phases, $\phi_{j,k} \equiv \pi/2$. Under this assumption, the Hamiltonian describing the system,

$$\hat{H}_1 = i \left[\frac{g_1}{2} (\hat{a}_1^{\dagger 2} - \hat{a}_1^2) + \frac{g_2}{2} (\hat{a}_2^{\dagger 2} - \hat{a}_2^2) \right] \hat{\sigma}_1, \quad (5)$$

yields an evolution operator,

$$\hat{U}_1(t) = \hat{S}_1(g_1 t \hat{\sigma}_1) \hat{S}_2(g_2 t \hat{\sigma}_1), \quad (6)$$

that is the product of two standard $SU(1, 1)$ squeezing operators, $\hat{S}_j(\alpha) = \exp \left[\alpha (\hat{a}_j^{\dagger 2} - \hat{a}_j^2) / 2 \right]$ controlled by the internal state of the trapped ion. For example, choosing an initial state with arbitrary phonon fields and the internal state an eigenstate of the $\hat{\sigma}_1$ operator, $|\psi(0)\rangle = |\xi_1, \xi_2, x_{\pm}\rangle$, the ideal evolution,

$$|\psi(t)\rangle = \hat{S}_1(\pm g_1 t) \hat{S}_2(\pm g_2 t) |\xi_1, \xi_2, x_{\pm}\rangle, \quad (7)$$

provides a separable state with different squeezing in each mode. These are the so-called two-mode $SU(1, 1)$ Perelomov coherent states [28]. Figure 1(a) shows the fidelity defined as the trace distance,

$$\mathcal{F}(t) = \text{Tr} [\hat{\rho}_{\psi}(t) \hat{\rho}_{\gamma}(t)], \quad (8)$$

between the density operator describing the ideal evolution, $\hat{\rho}_{\psi}(t) = |\psi(t)\rangle \langle \psi(t)|$, and that for evolution under atomic decay, $\hat{\rho}_{\gamma}(t)$ such that $\dot{\rho} = -i [\hat{H}, \hat{\rho}] + \gamma_q (\hat{\sigma}_- \hat{\rho} \hat{\sigma}_+ - \{\hat{\sigma}_+ \hat{\sigma}_-, \hat{\rho}\} / 2) + \sum_j \gamma_j (\hat{a}_j \hat{\rho} \hat{a}_j^{\dagger} - \{\hat{a}_j^{\dagger} \hat{a}_j, \hat{\rho}\} / 2)$ where γ_q and γ_j are the effective atomic and vibrational decay rates. The parameters in the simulations are $g_2 = 0.75 g_1$ and, for the sake of the example, homogeneous decays $\gamma_q = \gamma_j = \gamma = 0.1 g_1$. Figures 1(b) to Fig. 1(d) show the joint phonon number probability,

$$P_{n,m}(t) = \text{Tr} [|m, n\rangle \langle m, n| \hat{\rho}], \quad (9)$$

for ideal and Fig. 1(e) to Fig. 1(g) for lossy evolution at different times. We colored the probability bars and show only a small section of the plot to make comparison simpler.

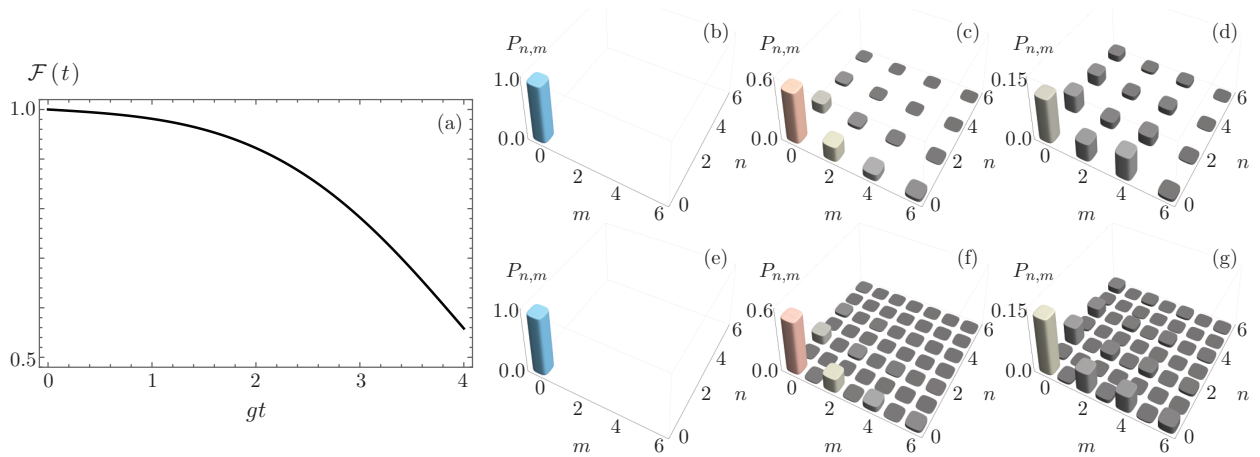


FIG. 1. (a) Fidelity between ideal evolution and evolution for asymmetric $SU(1,1)$ coherent states with $g_2 = 0.75 g_1$ and $\gamma = 0.1 g_1$. The joint phonon number probability distribution for (b)-(d) ideal and (e)-(g) lossy evolution at (b),(e) $g_1 t = 0$, (c),(f) $g_1 t = 1$, and (d),(g) $g_1 t = 2$.

Obviously, choosing an arbitrary internal initial state, $|\psi(0)\rangle = |\xi_1, \xi_2\rangle (\alpha|x_+\rangle + \beta|x_-\rangle)$, provides a superposition of the form,

$$|\psi(t)\rangle = \alpha \hat{S}_1(g_1 t) \hat{S}_2(g_2 t) |\xi_1, \xi_2, x_+\rangle - \beta \hat{S}_1^\dagger(g_1 t) \hat{S}_2^\dagger(g_2 t) |\xi_1, \xi_2, x_-\rangle, \quad (10)$$

where the state of the whole system is entangled thanks to the internal state of the ion. Figure 2(a) shows the fidelity between the ideal and lossy evolution. Figures 2(b) to Fig. 2(d) show the joint phonon number probability, for ideal and Fig. 2(e) to Fig. 2(g) for lossy evolution. Parameters are identical to those in Fig. 1.

The fact that a π -phase change in the driving laser phases ideally reverts the effective model dynamics might suggest its use as a squeezed state interferometer. In a real-world experiment, the system will not return to the original initial state due to all the real-world experimental subtleties. For example, these states might help in the characterization of the environment effect on the trapped center of mass motion and internal states of the ion might mention the obvious.

IV. SYMMETRIC SQUEEZING

Now, let us simplify our model one step more and assume a system where the coupling parameters, $g_{j,k} \equiv g$, and the phases are chosen to be equal. The dynamics are given by a simpler Hamiltonian that produces symmetric squeezing if we follow the procedure

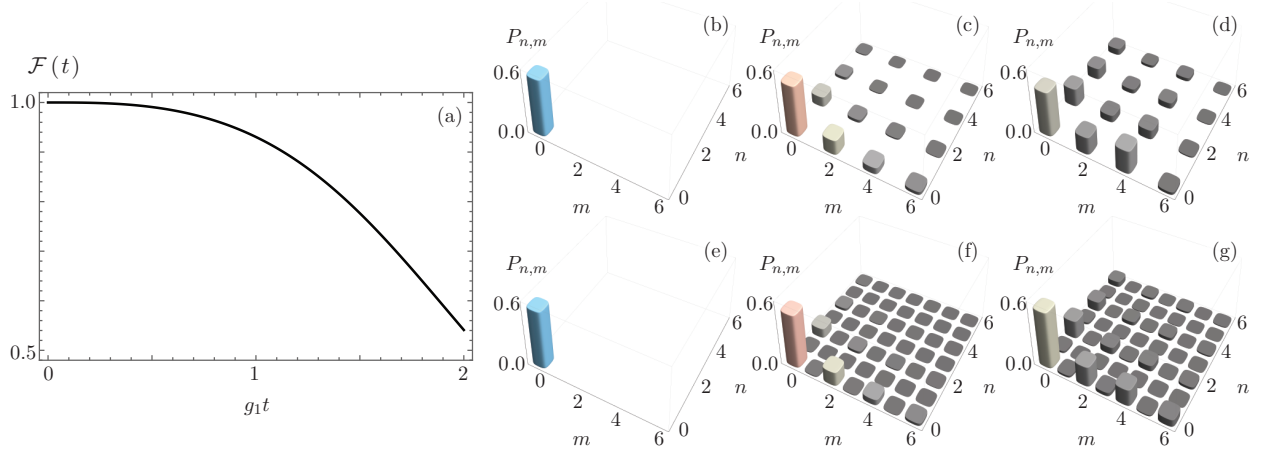


FIG. 2. (a) Fidelity between ideal evolution and evolution for asymmetric $SU(1, 1)$ coherent states with $g_2 = 0.75 g_1$ and $\gamma = 0.1 g_1$. The joint phonon number probability distribution for (b)-(d) ideal and (e)-(g) lossy evolution at (b),(e) $g_1 t = 0$, (c),(f) $g_1 t = 1$, and (d),(g) $g_1 t = 2$.

introduced before. We can take a second step and suppress blue sideband driving, then the dynamics are described by a Hamiltonian,

$$\hat{H}_2 = \frac{g}{2} \left[\left(\hat{a}_1^{\dagger 2} + \hat{a}_2^{\dagger 2} \right) \hat{\sigma}_- + \left(\hat{a}_1^2 + \hat{a}_2^2 \right) \hat{\sigma}_+ \right]. \quad (11)$$

Again, it is straightforward to construct an evolution operator,

$$\hat{U}_2(t) = \begin{pmatrix} \cos gt \sqrt{\hat{K}_- \hat{K}_+} & -i \sin gt \sqrt{\hat{K}_- \hat{K}_+} \frac{1}{\sqrt{\hat{K}_- \hat{K}_+}} \hat{K}_- \\ -i \hat{K}_+ \frac{1}{\sqrt{\hat{K}_- \hat{K}_+}} \sin gt \sqrt{\hat{K}_- \hat{K}_+} & \cos gt \sqrt{\hat{K}_+ \hat{K}_-} \end{pmatrix}, \quad (12)$$

using a representation of $SU(1, 1)$,

$$[\hat{K}_+, \hat{K}_-] = -2\hat{K}_3, \quad [\hat{K}_3, \hat{K}_{\pm}] = \pm \hat{K}_{\pm}, \quad (13)$$

provided by the two-mode operators [28],

$$\hat{K}_3 = \frac{1}{2} \left(\sum_{j=1}^2 \hat{a}_j^{\dagger} \hat{a}_j + 1 \right), \quad \hat{K}_+ = \frac{1}{2} \left(\hat{a}_1^{\dagger 2} + \hat{a}_2^{\dagger 2} \right), \quad \hat{K}_- = \frac{1}{2} \left(\hat{a}_1^2 + \hat{a}_2^2 \right). \quad (14)$$

We will use a Hilbert space partition defined by the raising operator,

$$|k; m\rangle = \sqrt{\frac{(2k-1)!}{m!(2k+m-1)!}} \hat{K}_+^m |k; 0\rangle, \quad (15)$$

acting on four states that we will call vacuum states related to a Bargmann index k . This produces four phonon subspaces labelled by a Bargmann index and a vacuum state: $k = 1/2$

and $|1/2; 0\rangle = |0, 0\rangle$, $k = 1$ and $|1; 0\rangle_{01} = |0, 1\rangle$, $k = 1$ and $|1; 0\rangle_{10} = |1, 0\rangle$, $k = 3/2$ and $|1, 0\rangle = |1, 1\rangle$. Figure 3 shows a pictorial representation of these phonon subspaces. The whole Hilbert state for the quantized center of mass motion is covered once with the four orthogonal subspaces defined by the bases,

$$\begin{aligned}
|1/2; m\rangle &= \frac{1}{2^m m!} \sum_{l=0}^m \binom{m}{l} \sqrt{(2m-2l)!(2l)!} |2m-2l, 2l\rangle, \\
|1; m\rangle_{01} &= \frac{1}{2^m} \sum_{l=0}^m \binom{m}{l} \sqrt{\frac{(2m-2l+1)!(2l)!}{m!(m+1)!}} |2l, 2m-2l+1\rangle, \\
|1; m\rangle_{10} &= \frac{1}{2^m} \sum_{l=0}^m \binom{m}{l} \sqrt{\frac{(2m-2l+1)!(2l)!}{m!(m+1)!}} |2m-2l+1, 2l\rangle, \\
|3/2; m\rangle &= \frac{1}{2^m} \sum_{l=0}^m \binom{m}{l} \sqrt{\frac{2(2m-2l+1)!(2l+1)!}{m!(m+2)!}} |2m-2l+1, 2l+1\rangle, \quad (16)
\end{aligned}$$

that are eigenstates of the \hat{K}_3 operator, $\hat{K}_3|k; m\rangle = (m+k)|k; m\rangle$.

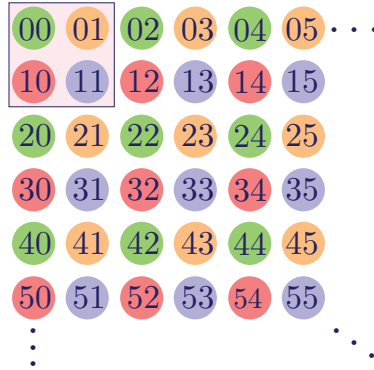


FIG. 3. Pictorial representation of the phonon subspaces; the vacuum state for each subspace are located within the marked square. Each color represents a given phonon subspace.

Here, we want to make a stop and remember the action of a lossless SU(2) beam splitter [10, 29],

$$\hat{T}(\theta) = \exp \left[i\theta \left(\hat{a}_1^\dagger \hat{a}_2 + \hat{a}_1 \hat{a}_2^\dagger \right) / 2 \right], \quad (17)$$

such that for a 50/50 beam splitter, $\theta = \pi/2$, we can rewrite the $SU(1, 1)$ bases above,

$$\begin{aligned}
|1/2; m\rangle &= \frac{(-i)^m}{m!} \hat{T}(\pi/2) \left(\hat{a}_1^{\dagger m} \hat{a}_2^{\dagger m} \right) \hat{T}^\dagger(\pi/2) |0, 0\rangle, \\
|1; m\rangle_{01} &= \frac{(-i)^m}{\sqrt{2m!(m+1)!}} \hat{T}(\pi/2) \left(\hat{a}_1^{\dagger m+1} \hat{a}_2^{\dagger m} - i \hat{a}_1^{\dagger m} \hat{a}_2^{\dagger m+1} \right) \hat{T}^\dagger(\pi/2) |0, 0\rangle, \\
|1; m\rangle_{10} &= \frac{(-i)^m}{\sqrt{2m!(m+1)!}} \hat{T}(\pi/2) \left(\hat{a}_1^{\dagger m} \hat{a}_2^{\dagger m+1} - i \hat{a}_1^{\dagger m+1} \hat{a}_2^{\dagger m} \right) \hat{T}^\dagger(\pi/2) |0, 0\rangle, \\
|3/2; m\rangle &= \frac{(-i)^{m+1}}{\sqrt{2m!(m+2)!}} \hat{T}(\pi/2) \left(\hat{a}_1^{\dagger m+2} \hat{a}_2^{\dagger m} - i \hat{a}_1^{\dagger m} \hat{a}_2^{\dagger m+2} \right) \hat{T}^\dagger(\pi/2) |0, 0\rangle, \quad (18)
\end{aligned}$$

in terms of ideal 50/50 beam splitter states. We have in our hands four phonon subspaces with an underlying $SU(1, 1)$ symmetry that resolves the Hilbert spaces of a lossless 50/50 $SU(2)$ beam splitter.

Now, let's go back to the ideal evolution of the model and consider an initial state composed by the m -th state in any of the $SU(1, 1)$ subspaces and the ion in the excited state, $|\psi(0)\rangle = |k, m\rangle|e\rangle$. It is straightforward to see,

$$|\psi(t)\rangle = \cos gt \sqrt{(m+1)(m+2k)} |k; m\rangle|e\rangle - i \sin gt \sqrt{(m+1)(m+2k)} |k; m+1\rangle|g\rangle \quad (19)$$

that we can scale the $SU(1, 1)$ state ladder by a sequence of red second sideband driving and π -pulses, $R_y(\pi) = \exp(i\pi\sigma_1/2)$, to switch the internal state of the ion,

$$\begin{aligned}
t = 0 & : |k; 0\rangle|e\rangle, \\
U_2\left(\frac{\pi}{2g\sqrt{2k}}\right) & : |k; 1\rangle|g\rangle, \\
e^{i\frac{\pi}{2}\sigma_1} & : |k; 1\rangle|e\rangle, \\
U_2\left(\frac{\pi}{2g\sqrt{2(2k+1)}}\right) & : |k; 2\rangle|g\rangle, \\
e^{i\frac{\pi}{2}\sigma_1} & : |k; 2\rangle|e\rangle, \\
U_2\left(\frac{\pi}{2g\sqrt{3(2k+2)}}\right) & : |k; 3\rangle|g\rangle,
\end{aligned} \quad (20)$$

and so on. Now, this procedure generates entangled orthogonal vibrational states that are factorized from the internal structure of the ion. Again, this result suggests the use of this system as an interferometer that might provide information about the characteristics of an experiment that might be, in principle, different from those available through the superposition of squeezed states proposed before.

Figure 4(a) shows the fidelity, $\mathcal{F}(t)$, between the ideal evolution of the driving algorithm in Eq.(20) and lossy evolution under homogeneous decay for all components. The initial state

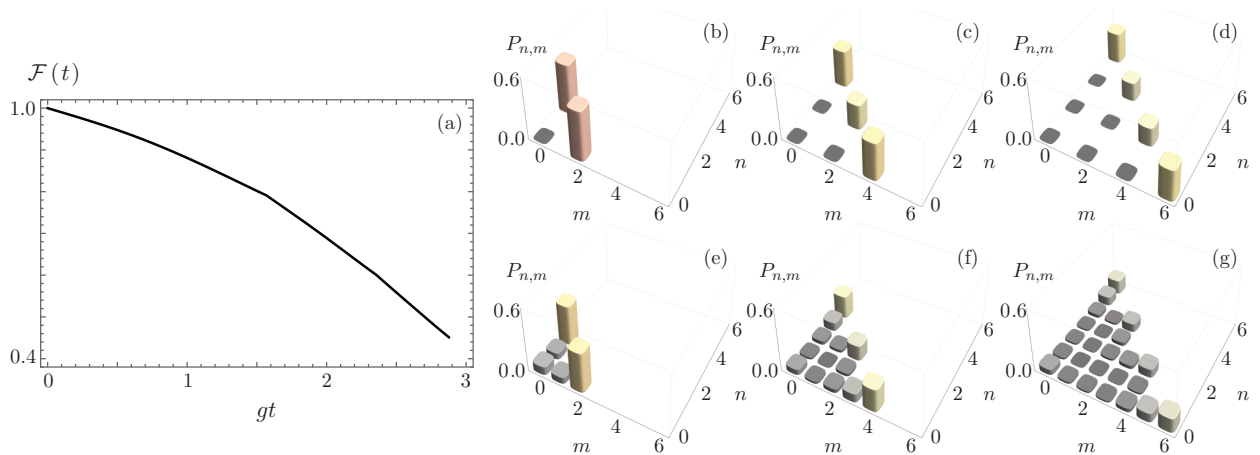


FIG. 4. (a) Fidelity between ideal evolution and evolution under a common decay rate $\gamma = 0.1 g$ for the symmetric coupling case, $g_1 = g_2 = g$. The joint phonon number probability distribution for times where 50/50 SU(2) beam splitter states are expected under (b)-(d) ideal and (e)-(g) lossy evolution for the SU(1,1) subspace characterized by Bargmann parameter $k = 1/2$ with (b),(e) $m = 1$, (c),(f) $m = 2$, and (d),(g) $m = 3$.

of the algorithm is the vacuum state for the subspace defined by the Bargmann parameter $k = 1/2$. That is, the initial state is the ion in the excited state and both vibrational modes cooled down to the vacuum state. Figures 4(b) to 4(d) show the joint phonon number probability, $P_{n,m}$, at times where the 50/50 SU(2) beam splitter states are expected under ideal time evolution. Figures 4(e) to 4(g) show the same probabilities for lossy evolution.

V. CONCLUSION

We proposed a trapped ion model under second sideband resolved blue and red driving of two orthogonal modes of the center mass motion in the Lamb-Dicke regime. For parameter regimes providing an effective model with asymmetric coupling of the vibration modes with the internal state of the ion, we showed that time evolution of arbitrary vibrational states with balanced superposition of the internal states of the ion generates a so-called two-mode SU(1,1) Perelomov coherent state where the vibrational modes are separable. Uneven superposition of the internal states of the ion produces a superposition where entanglement of the whole state of the ion arises. We also showed that under red driving only, the effective model is able to generate 50/50 SU(2) beam splitter vibrational states factorized from the

internal state of the ion. The fact that it is ideally possible to engineer these states with reversible dynamics suggests the use of these models as interferometers to characterize real-world experiments.

ACKNOWLEDGMENTS

C.H.A. acknowledges funding through CONACYT 455378 doctoral studies grant. M. P. M. R. acknowledges financial support through the Verano de Investigación Científica program from Academia Mexicana de Ciencias. B.M.R.L. acknowledges funding from CONACYT through CB-2015-01-255230 and FORDECYT-296355 project grants.

-
- [1] D. J. Wineland, C. Monroe, W. M. Itano, D. Leibfried, B. E. King, and D. M. Meekhof, “Experimental issues in coherent quantum-state manipulation of trapped atomic ions,” *J. Res. Natl. Inst. Stand. Tech.* **103**, 259 – 328 (1998), [arXiv:9710025 \[quant-ph\]](#).
 - [2] D. Leibfried, D. M. Meekhof, B. E. King, C. Monroe, W. M. Itano, and D. J. Wineland, “Experimental Determination of the Motional Quantum State of a Trapped Atom,” *Phys. Rev. Lett.* **77**, 4281–4285 (1996).
 - [3] D. Lv, S. An, M. Um, J. Zhang, J.-N. Zhang, M. S. Kim, and K. Kim, “Reconstruction of the Jaynes-Cummings field state of ionic motion in a harmonic trap,” *Phys. Rev. A* **95**, 043813 (2017).
 - [4] D. Kielpinski, C. Monroe, and D. J. Wineland, “Architecture for a large-scale ion-trap quantum computer,” *Nature* **417**, 709 – 711 (2002).
 - [5] R. Blatt and C. F. Roos, “Quantum simulations with trapped ions,” *Nature Physics* **8**, 277–284 (2012).
 - [6] D. M. Meekhof, C. Monroe, B. E. King, W. M. Itano, and D. J. Wineland, “Generation of Nonclassical Motional States of a Trapped Atom,” *Phys. Rev. Lett.* **76**, 1796–1799 (1996).
 - [7] C. K. Law and J. H. Eberly, “Arbitrary Control of a Quantum Electromagnetic Field,” *Phys. Rev. Lett.* **76**, 1055–1058 (1996).
 - [8] G. Drobn, B. Hladk, and V. Buek, “Quantum-state synthesis of multimode bosonic fields: Preparation of arbitrary states of two-dimensional vibrational motion of trapped ions,” *Phys.*

- Rev. A* **58**, 2481–2487 (1998), [arXiv:9801008 \[quant-ph\]](#).
- [9] S.-C. Gou and P. L. Knight, “Trapped ions as vibrational beam splitters: $SU(2)$ states in a two-dimensional ion trap,” *Phys. Rev. A* **54**, 1682–1690 (1996).
 - [10] R. A. Campos, B. E. A. Saleh, and M. C. Teich, “Quantum-mechanical lossless beam splitter: $SU(2)$ symmetry and photon statistics,” *Phys. Rev. A* **40**, 1371–1384 (1989).
 - [11] J. F. Poyatos, J. I. Cirac, R. Blatt, and P. Zoller, “Trapped ions in the strong-excitation regime: Ion interferometry and nonclassical states,” *Phys. Rev. A* **54**, 1532–1540 (1996), [arXiv:9509007 \[quant-ph\]](#).
 - [12] H. Zeng, “Motional wave-packet splitting and ion-trap interferometry,” *Phys. Rev. A* **57**, 388–391 (1998).
 - [13] K. G. Johnson, B. Neyenhuis, J. Mizrahi, J. D. Wong-Campos, and C. Monroe, “Sensing Atomic Motion from the Zero Point to Room Temperature with Ultrafast Atom Interferometry,” *Phys. Rev. Lett.* **115**, 213001 (2015), [arXiv:1507.06591 \[quant-ph\]](#).
 - [14] W. C. Campbell and P. Hamilton, “Rotation sensing with trapped ions,” *J. Phys. B: At. Mol. Opt. Phys.* **50**, 064002 (2017), [arXiv:1609.00650 \[physics.atom-ph\]](#).
 - [15] B. Yurke, S. L. McCall, and J. R. Klauder, “ $SU(2)$ and $SU(1,1)$ interferometers,” *Phys. Rev. A* **33**, 4033–4054 (1986).
 - [16] B. Bhmer and U. Leonhardt, “Correlation interferometer for squeezed light,” *Opt. Commun.* **118**, 181–185 (1995).
 - [17] R. Carranza and C. C. Gerry, “Photon-subtracted two-mode squeezed vacuum states and applications to quantum optical interferometry,” *J. Opt. Soc. Am. B* **29**, 2581–2587 (2012).
 - [18] R. L. de Matos Filho and W. Vogel, “Second-sideband laser cooling and nonclassical motion of trapped ions,” *Phys. Rev. A* **50**, R1988–R1991 (1994).
 - [19] R. L. de Matos Filho and W. Vogel, “Even and Odd Coherent States of the Motion of a Trapped Ion,” *Phys. Rev. Lett.* **76**, 608–611 (1996).
 - [20] A. Messina, S. Maniscalco, and A. Napoli, “Interaction of bimodal fields with few-level atoms in cavities and traps,” *J. Mod. Opt.* **50**, 1–49 (2003), [arXiv:0206155 \[quant-ph\]](#).
 - [21] S.-L. Zhu, C. Monroe, and L.-M. Duan, “Trapped Ion Quantum Computation with Transverse Phonon Modes,” *Phys. Rev. Lett.* **97**, 050505 (2006), [arXiv:0601159 \[quant-ph\]](#).
 - [22] W. Vogel and R. L. de Matos Filho, “Nonlinear Jaynes-Cummings dynamics of a trapped ion,” *Phys. Rev. A* **52**, 4214–4217 (1995).

- [23] J. S. Pedernales, I. Lizuain, S. Felicetti, G. Romero, L. Lamata, and E. Solano, “Quantum Rabi Model with Trapped Ions,” [Sci. Rep. **5**, 15472 \(2015\)](#), [arXiv:1505.00698 \[quant-ph\]](#).
- [24] D. Lv, S. An, Z. Liu, J.-N. Zhang, J. S. Pedernales, L. Lamata, E. Solano, and K. Kim, “Quantum Simulation of the Quantum Rabi Model in a Trapped Ion,” [Phys. Rev. X **8**, 021027 \(2018\)](#), [arXiv:1711.00582 \[quant-ph\]](#).
- [25] C. Huerta Alderete and Rodríguez-Lara. B. M., “Cross-cavity quantum Rabi model,” [J. Phys. A: Math. Theor. **49**, 414001 \(2016\)](#), [arXiv:1604.04012 \[quant-ph\]](#).
- [26] C. Huerta Alderete and B. M. Rodríguez-Lara, “Quantum simulation of driven para-Bose oscillators,” [Phys. Rev. A **95**, 013820 \(2017\)](#), [arXiv:1609.09166 \[quant-ph\]](#).
- [27] C. Huerta Alderete and B. M. Rodríguez-Lara, “Simulating para-Fermi oscillators,” [Sci. Rep. **8**, 11572 \(2018\)](#), [arXiv:1803.00654 \[quant-ph\]](#).
- [28] C. C. Gerry and A. Benmoussa, “Two-mode coherent states for $SU(1,1) \otimes SU(1,1)$,” [Phys. Rev. A **62**, 033812 \(2000\)](#).
- [29] A. Luis and L. L. Sanchez-Soto, “A quantum description of the beam splitter,” [Quantum and Semiclass. Opt.: Journal of the European Optical Society Part B **7**, 153 \(1995\)](#).